

Ulrich Sauter
17-935-966

Gain characterization of pump DBR VECSEL in the 2- μm range

Semester project

Ultrafast Laser Physics, Prof. Ursula Keller
Department of Physics, Institute for Quantum Electronics
Swiss Federal Institute of Technology Zürich

Supervision

Marco Gaulke

May, 2023

Abstract

A novel optically-pumped vertical external cavity surface emitting laser (VECSEL) operating in the 2 μm spectral range

In order to gain deeper insights into the impact of VECSEL design (?MENTION WHAT CHANGES IN DESIGN?), it is necessary to measure the characteristic parameters of the VECSEL under various conditions. This involved utilizing an existing setup and control software to measure these parameters at various temperatures and pump powers. To enhance efficiency and save valuable measurement time, the setup was further improved by adding the possibility to control and automate the pump diode power, as well as further improvement to the stability and detection algorithm of the software.

Contents

Abstract	I
1 Introduction	1
1.1 Gain saturation	2
2 Methods	4
2.1 VECSEL Chips	4
2.2 Experimental setup	6
2.2.1 Automation of the pump power	8
2.3 Data processing	9
3 Results and Discussion	10
3.1 Measurement results	10
3.1.1 Saturation fluence F_{sat}	10
3.1.2 Small signal Reflectivity R_{ss}	10
3.1.3 Roll over parameter F_2	10
3.1.4 Overview	10
4 Conclusion and Outlook	12

Chapter 1

Introduction

Semiconductor lasers present a very compact compact, efficient and massproducible solid state laser. They have many applications in everyday life and science, such as optical communication, data storage, printing, sensing, medical treatment, and pumping solid-state lasers.

A special type of semiconductor laser is a VECSEL (Vertical External Cavity Surface Emitting Laser). It is based on a VCSEL (Vertical Cavity Surface Emitting Laser) and emits light perpendicular to the surface of a semiconductor wafer but unlike a VCSEL, a VECSEL has an external cavity that is formed by one or more optical elements outside the wafer. This allows for more flexibility in designing the laser parameters, such as wavelength, output power, beam quality and pulse duration.

The basic structure of the VECSEL itself consists of an active region and a distributed Bragg reflector (DBR). Inside the active region, multiple quantum wells are located which are engineered to provide the necessary energy levels for the desired wavelength of laser emission, in this case the 2- μm range. This wavelength range is of strong interest for many application, particularly for medical purposes and atmospheric spectroscopy. The DBR is made of alternating layers of semiconductor material with different refractive indices. By choosing the layer thicknesses to be one quarter of the laser wavelength, the DBR achieves high reflectivity at the desired wavelength range of the laser.

A novel design approach incorporates a DBR for the pump wavelength as well. This new structure shows remarkable improvements in terms of efficiency and power scaling in continuous wave (CW) operation, as seen in Fig. 1.1. The performance improvements in a modelocked configuration were not as significant. To get a better understanding of this, additional investigation were conducted and for this work we focused on the gain saturation characteristics.

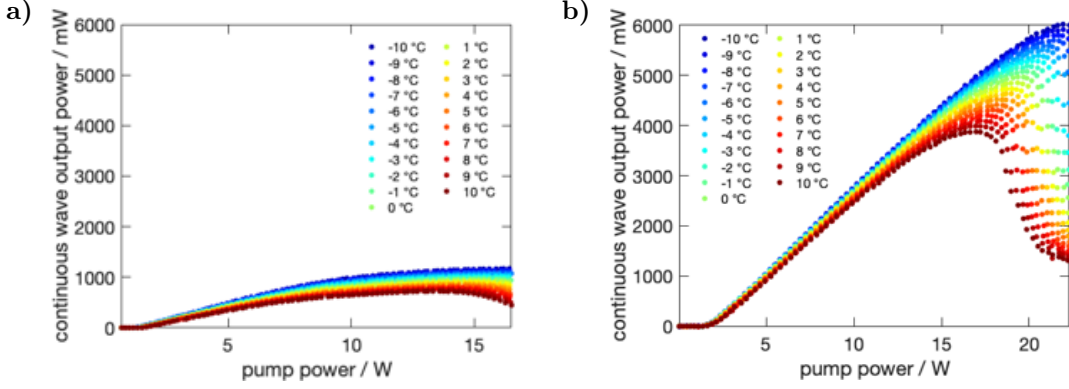


Figure 1.1: Continuous wave (CW) output power of a VECSEL without pump DBR a) and with pump DBR b) versus pump power under different heatsink temperature ranging from -10°C to 10°C . The data demonstrates the effect of the pump DBR on the power scaling performance in CW operation. The VECSEL with pump DBR shows an increase of 18 % and a sixfold increase in output power.

1.1 Gain saturation

Gain saturation describes a phenomenon that occurs when the active region of a laser is unable to maintain its gain as the pump power increases for high values.

To study this behavior, one measures the nonlinear behavior of the reflectivity for an increasing amount of probe fluence, as can be seen in Fig. 1.2. To quantify this behavior and gain some macroscopic parameters, a model based on the saturation of the absorber in a SESAM can be fitted to the data.

$$R(F) = R_{ns} \frac{F_{sat}}{F} \ln \left\{ 1 + \frac{R_{ss}}{R_{ns}} \left[\exp \left(\frac{F}{F_{sat}} \right) - 1 \right] \right\} \exp \left(-\frac{F}{F_2} \right) \quad (1.1)$$

The parameters from Eq. (1.1) are the saturation fluence F_{sat} , the small signal reflectivity R_{ss} , the nonsaturable reflectivity R_{ns} and the rollover parameter F_2 .

The saturation fluence F_{sat} is the fluence at which the reflectivity reduces to $1/e$ of its maximum. It also represents the point at which the population inversion inside the active region becomes saturated, therefore it is closely tied to the material properties of the active region.

The small signal reflectivity R_{ss} refers to the reflectivity at low probe fluence, where the gain is not significantly saturated. In this regime nonlinear effects are minimal and the reflectivity can be considered to be in the linear regime and the small signal approximation can be applied and the small signal gain can be calculated as $g_{ss} = R_{ss} - 100\%$.

The nonsaturable reflectivity R_{ns} arises from absorption and scattering at impurities and interfaces inside the VECSEL structure. This limits the maximum

performance of the VECSE, thus reducing defect during the growing process is important. Since this effect is associated with imperfection and reflection inside the structure it remains relatively constant for different probe fluences.

The rollover parameter F_2 describes further absorption from two photon absorption or higher order effects resulting in a strong decrease in the reflectivity at high fluences.

Figure 1.2 shows the key parameters and the fitted model with and without accounting for the rollover for a measurement of a VECSEL with an integrated pump DBR.

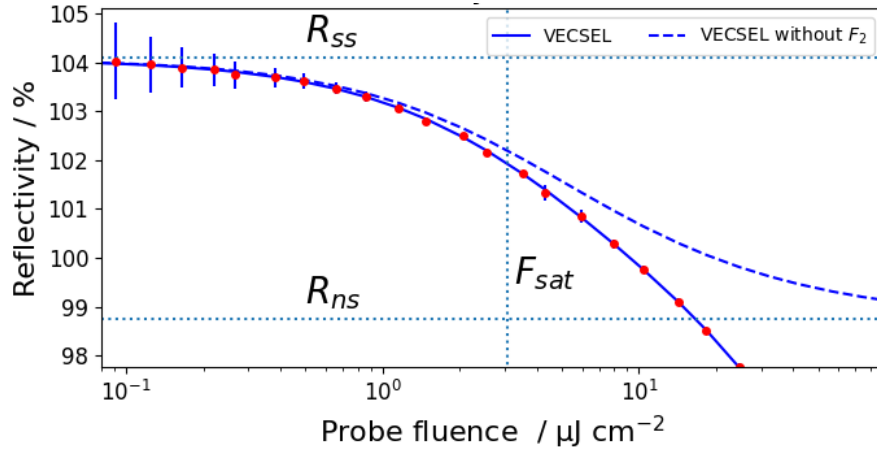


Figure 1.2: Nonlinear reflectivity measurement for a diamond backed VECSEL with integrated pump DBR versus probe fluence. The data is shown with the fitted model utilizing Eq. (1.1) and the same model without the roll over parameter F_2 . Additionally the different parameters R_{ss} , R_{ns} and F_{sat} are visualized.

Chapter 2

Methods

In order to accurately determine the characteristic parameters of a VECSEL chip, it is necessary to have an experimental setup that can measure a small change, in the order of 0.1% in the reflectivity over a dynamic range of about 4 order of magnitude in pulse fluence. A dedicated setup fulfilling these criteria has been constructed and utilized by (INSERT HERE REFERENCES).

For the measurements, a total of 4 different VECSEL chips were used, with three of them having a different structure (further discussed in Section 2.1). We were interested in the impact of different pump powers and the temperatures on the characteristic parameters of the VECSEL across the three different structures. For this we measured the nonlinear reflectivity for each chip for 9 different pump powers in the range from 0 W to 32 W and for three temperatures -10°C , 0°C and 10°C .

The subsequent section provides an overview of the different VECSEL structures, the measurement setup and the data processing method.

2.1 VECSEL Chips

TODO: redo design images maybe with legend? different colors?

The basic structure of a VECSEL gain chip is shown in Fig. 2.1. The main features of the structure are as follows:

- Heat spreader: The heat spreader role is in dissipating the heat generated during the operation of the VECSEL chip to a Peltier-controlled copper heat-sink.
- Pump & laser DBR: The purpose of the two bottom mirrors is to reflect the laser light and the pump light. There are two main advantages to this

approach: firstly, because of higher absorption, there is a higher optical-to-optical efficiency due to the two passes through the active region, and secondly, there is less absorption in the mirror and in the heat sink, which results also in a higher efficiency and a higher maximum output power. The high reflectivity for two wavelengths is realized by using a distributed Bragg reflector (DBR)

- Active region: The purpose of the active region is the conversion of the pump light into the laser light. The gain medium in the active region is often composed of quantum wells or quantum dots.
- Anti-reflection coating: The antireflection section is optimized to reduce the otherwise large reflection from the air/GaAs interface

Below the three different structure of the Vecsel chips used in this work.

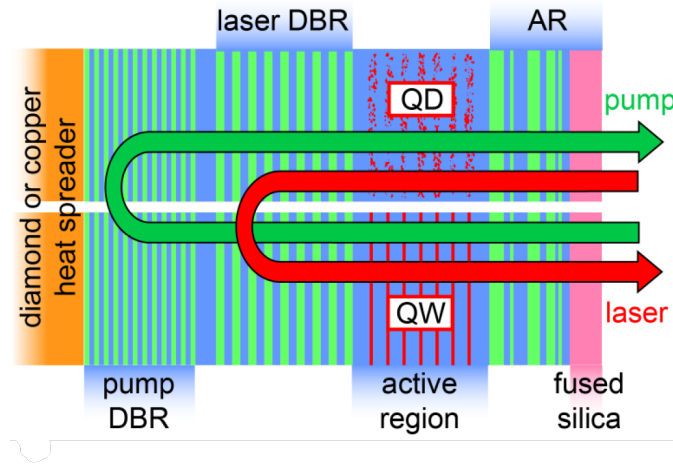


Figure 2.1: TODO: caption

No pump DBR chip, SV166

This structure has an antiresonant design and cooled from the backside by a copper heat spreader. The DBR consists of 19-pairs of $\text{GaSb}/\text{AlAs}_{0.08}\text{Sb}_{0.92}$ layers design around a wavelength of 2080 nm. The active region has 5×3 $\text{In}_{0.27}\text{Ga}_{0.73}\text{Sb}$ quantum wells (QW) placed at the maximum of the standing-wave cavity. Additional barriers layer made of $\text{AlAs}_{0.08}\text{Sb}_{0.92}$ are placed around the gain QW to increase the photoluminescence. The last layer is a PECVD coating made of Si_3N_4 , which serves an an antireflection coating.

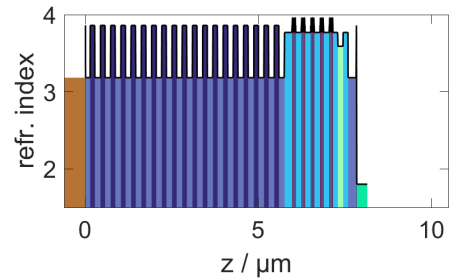


Figure 2.2: TODO: caption

Pump DBR chip, SV167

This is a similar structure as above but this time including an extra DBR for the pump wavelength of 1470 nm. The pump DBR is made of 10 layers of $\text{Al}_{0.2}\text{As}_{0.8}\text{Sb}/\text{Al}_{0.15}\text{Ga}_{0.85}\text{AsSb}$. For the thickness of the layers the 45° incident of the pump beam had to be accounted for. This structure was measured twice but for different heat spreaders, one made of copper and the other of diamond, to observe and compare the influence of better thermal conductivity of the heatsinks.

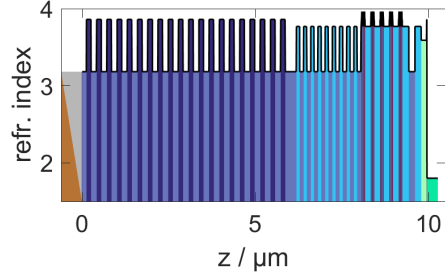


Figure 2.3: TODO: caption

Hybrid chip, SV165

This structure incorporated a hybrid metal-semiconductor Bragg reflector. It consisted of a 100 nm copper layer with 10.5 $\text{AlAs}_{0.08}\text{Sb}_{0.92}/\text{GaSb}$ layers. This allows for a thinner gain chip design of just under $5\mu\text{m}$ compared to the other structures $7.5\mu\text{m}$ resp. $10\mu\text{m}$ for the pump DBR design. This lowered the thermal resistance of the device by 24%. This structure also has a different active region made of $5 \times 3 \text{ In}_{0.27}\text{Ga}_{0.73}\text{Sb}/\text{GaSb}$ QW.

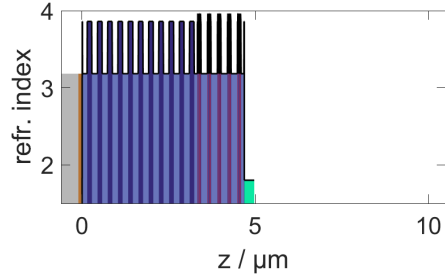


Figure 2.4: TODO: caption

2.2 Experimental setup

The experimental setup is depicted in Fig. 2.5. The setup is driven by a mode-locked Ti:sapphire laser. The laser emits femtosecond pulses at a wavelength of 810 nm, with a repetition rate of 80 MHz and an average output power of 4 W. The laser beam then passes through an optical parametric oscillator (OPO), where the beam undergoes nonlinear frequency conversion resulting in two waves: an idler wave and a signal wave. The OPO idler wave can be tuned from $1.7\mu\text{m}$ to $4\mu\text{m}$ and has a maximum output power of 650 mW. The idler has been tuned to a specific wavelength of 2071.7 nm and was stabilized using an integrated automated feedback loop.

To further achieve a wide range of pulse fluences, the laser beam is directed through two wire-grid polarizers. One of the polarizers is placed on a controllable rotation stage to adjust the beam attenuation. The wire-grid polarizers have a broad range of attenuation across different wavelengths and do not alter the beam

path during rotation. After the attenuation stage, the beam passes through a beamsplitter, which separates it into two arms: the reference arm and the sample arm.

The reference arm contains a high-reflection mirror, from which a portion of the beam is leaked and collected by a photodiode. The reference arm contains a high-reflection mirror from which the leaking signal is collected in a photo diode to monitor the fluence during a measurement. The sample in this experiment refers to a VECSEL chip and is placed at the end of the sample arm. Before the beam is incident on the sample, a focusing lens is used to achieve higher fluences on the VECSEL. The VECSEL is probed under a direct incidence angle, and its reflection is collected using the same lens. Both beams are recombined at the beamsplitter and directed to an integrating sphere photodiode to measure the total reflected power. The pump beam enters from the side at a 30° angle and is shown in green.

To differentiate the signals from the two different arms and also measure the photoluminescence (PL) signal of the pumped VECSEL chips, two choppers are used. The two choppers are phase locked and chopper 2 is run at half of the frequency of chopper 1, specifically at 55 Hz. Chopper 2 is placed in the beam path before the attenuator to block the beam during every second cycle of chopper 1. This configuration allows to isolate the PL signal. Whereas chopper 1 is placed such that both arms pass through the blades, enabling the passage of light from both or either of the arms.

TODO: The measurement part consists of a non-polarizing beam splitter cube (BS), a lens, a chopper wheel and a photo detector (PD). Instead of detecting A and B simultaneously by two different detectors (like Haiml et al [16]), the signals are separated in time and measured with the same detector system. The separation in time is achieved by a chopper wheel which simultaneously chops both arms and is put close to the 50:50 beamsplitter. The signal is amplified and measured with an analog-to-digital (AD) converter and recorded with a computer. The chopper frequency is typically in the range of 100s of Hertz, and a low-cost 14 bit AD-converter is sufficient to measure photovoltages with 0.01% accuracy (when the photo-current amplifier is set to obtain a full-scale for the reference signal, 14 bits results in 0.006% resolution, averaging over more points can even increase this value). In our measurement system, we lifted the chopper wheel such that the axis of the chopper wheel is a few centimeters above the beam heights, see Fig. 4(a). During one chopper wheel cycle, four different states occur: 1. only reference beam measured, 2. both beams measured, 3. only sample beam measured, and 4. both beams are blocked. The signal in phase 4 corresponds to a background signal from photodiode dark current and environmental background light, which is then discriminated from the measurement signal in phase 1 and 3. In reference [16], a lock-in detection was required to reject the background signal. The lens L1 focuses the incident beam onto the SESAM, typical beam radii are between 5 μm and 20 μm . We employ a photo detector with a large detection area (typically 7×7

mm) to measure a collimated beam with large beam radius.

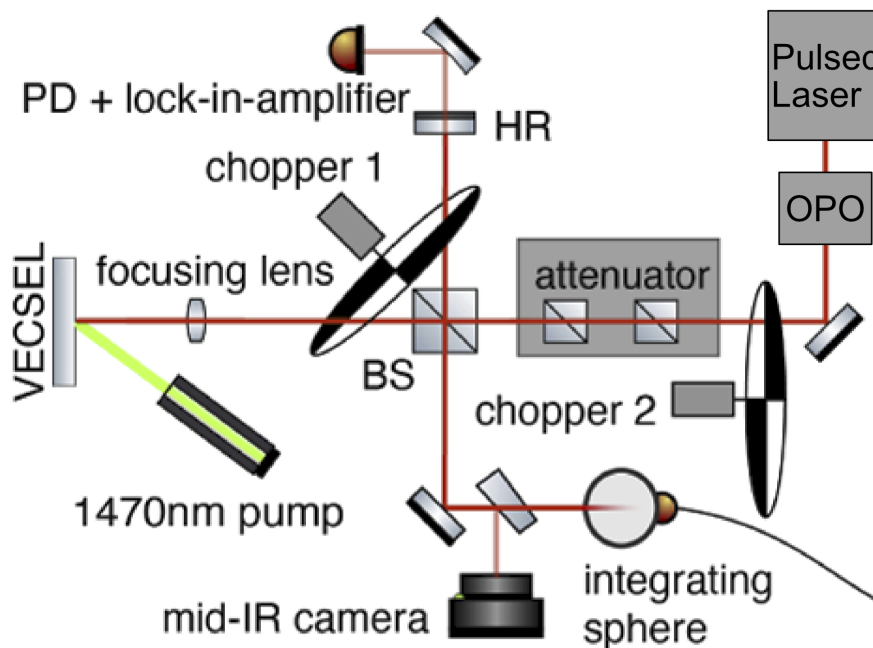


Figure 2.5: Experimental Setup for gain characterization of VECSEL chips. The laser source is a tunable optical parametric oscillator pumped by a modelocked Ti:sapphire laser. The beam gets attenuated. The pump beam enters the setup at a 30° angle. Two choppers, phase-locked and operating at different frequencies, are positioned to differentiate signals and measure photoluminescence (PL) emitted by the pumped VECSEL chips. The figure showcases the key components and their relative positions within the experimental setup.

2.2.1 Automation of the pump power

In the original setup, the pump laser diode was controlled over a DC power supply, which can deliver up to 50 A at up to 18 V. The power supply was operated manually in a current control mode. This required after

Due to the choice of measuring for 9 different pump powers for each temperature and chip design and one measurement taking about 10 min. All the measurements would take a significant amount of time without much downtime between the measurements, since each measurement required to change the pump power and also to manually start the measurement. Fortunately the power supply had a serial interface, which could be controlled from the software, it was only necessary to build in. This allowed to additionally set up the current control for the pump power and measure the pump power in one go taking about 90 min.

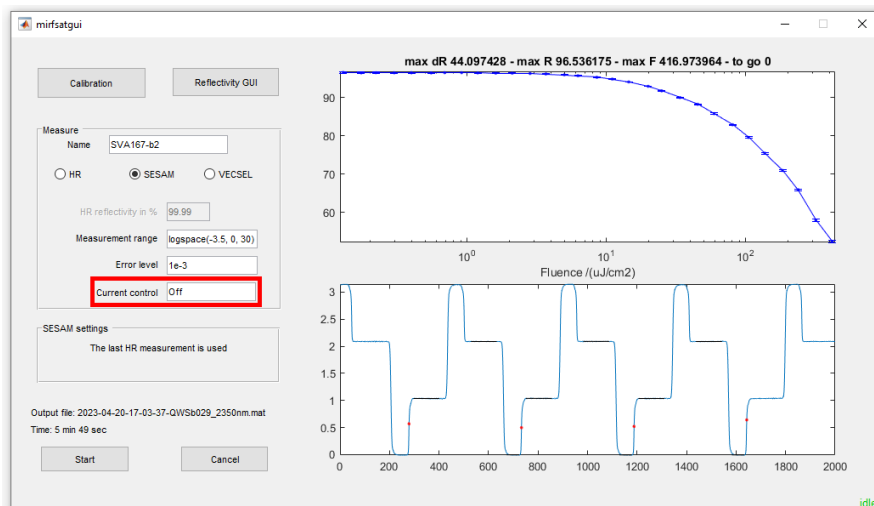


Figure 2.6

2.3 Data processing

The PD signal is amplified by a computer-controlled variable pre-amplifier to use the full range of the AD converter. The absolute gain and the offset have no influence on the measurement accuracy, it is only necessary to provide a linear response. Since the reflectivity R is encoded in only one optical/electrical signal the constraints on the amplifier have become negligible. This is in contrast to the method of Haiml et al., in which the same gain and no offset has to be achieved by both amplifiers [16]. The computer algorithm first detects the rising edges (red dots in Fig. 4(c)) and then takes the mean value of the data points on the flat levels (red lines in Fig. 4(b)). As both beams are blocked in phase 4, we can precisely measure the offset of the photodiode. Level A and B (Fig. 4(b)) are obtained by subtracting the signal level in state 1, and the nonlinear reflectivity is obtained as $R = B / A$. This is done for 500 periods in succession (takes approximately 5 seconds per fluence) and averaged to minimize detector noise and laser noise. This averaged reflectivity has a standard deviation of 0.01%. The incident fluence can be computed from the level A and the pre-amplifier gain setting. An accuracy of 5% for the fluence measurement is typically good enough, as this will afterwards result in an inaccuracy of 5% for the fitted saturation fluence F_{sat} .

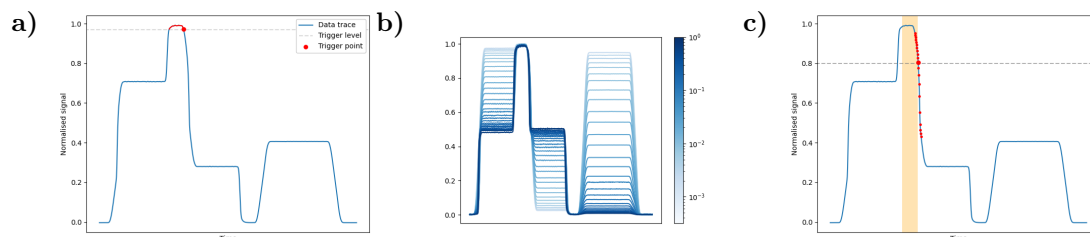


Figure 2.7: Main caption

Chapter 3

Results and Discussion

3.1 Measurement results

3.1.1 Saturation fluence F_{sat}

3.1.2 Small signal Reflectivity R_{ss}

3.1.3 Roll over parameter F_2

3.1.4 Overview

In Fig. 3.1 the result of the 0 °C measurement can be seen.

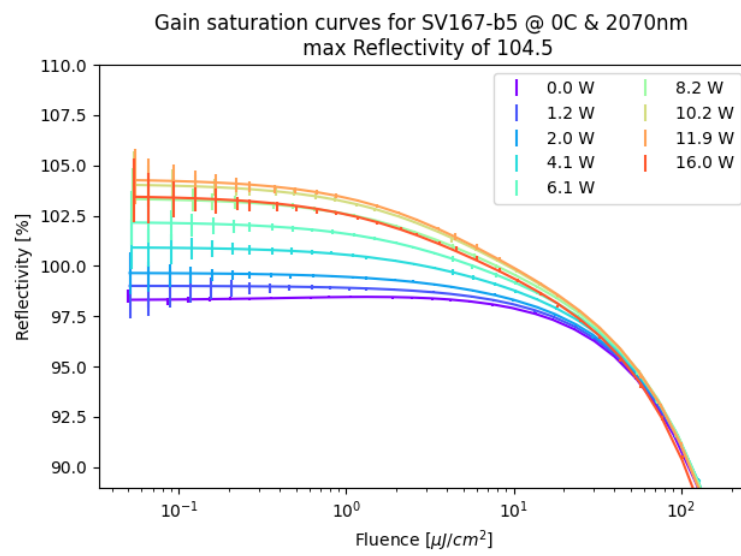


Figure 3.1

Chapter 4

Conclusion and Outlook